

Surface-emitting dye-doped polymer laser coupled with stimulated resonant Raman scattering

Hisao Yanagi, Hidetaka Miyamoto, Atsushi Ishizumi, Satoshi Tomita, Kenichi Yamashita et al.

Citation: *Appl. Phys. Lett.* **96**, 263304 (2010); doi: 10.1063/1.3459967

View online: <http://dx.doi.org/10.1063/1.3459967>

View Table of Contents: <http://apl.aip.org/resource/1/APPLAB/v96/i26>

Published by the [American Institute of Physics](http://www.aip.org).

Related Articles

Buried-heterostructure quantum-cascade laser overgrown by gas-source molecular-beam epitaxy
Appl. Phys. Lett. **100**, 213504 (2012)

High power, continuous wave, room temperature operation of λ 3.4 μ m and λ 3.55 μ m InP-based quantum cascade lasers
Appl. Phys. Lett. **100**, 212104 (2012)

Improved terahertz quantum cascade laser with variable height barriers
J. Appl. Phys. **111**, 103106 (2012)

Thermal characterization of GaN-based laser diodes by forward-voltage method
J. Appl. Phys. **111**, 094513 (2012)

Model for direct-transition gain in a Ge-on-Si laser
Appl. Phys. Lett. **100**, 191113 (2012)

Additional information on *Appl. Phys. Lett.*

Journal Homepage: <http://apl.aip.org/>

Journal Information: http://apl.aip.org/about/about_the_journal

Top downloads: http://apl.aip.org/features/most_downloaded

Information for Authors: <http://apl.aip.org/authors>

ADVERTISEMENT



Goodfellow
metals • ceramics • polymers • composites
70,000 products
450 different materials
small quantities fast

www.goodfellowusa.com

Surface-emitting dye-doped polymer laser coupled with stimulated resonant Raman scattering

Hisao Yanagi,^{1,a)} Hidetaka Miyamoto,¹ Atsushi Ishizumi,¹ Satoshi Tomita,¹ Kenichi Yamashita,² and Kunishige Oe²

¹Graduate School of Materials Science, Nara Institute of Science and Technology (NAIST), 8916-5 Takayama-cho, Ikoma, Nara 630-0192, Japan

²Department of Electronics, Graduate School of Science and Technology, Kyoto Institute of Technology, Matsugasaki Goshokaidocho, Sakyo-ku, Kyoto 606-8585, Japan

(Received 25 March 2010; accepted 13 June 2010; published online 1 July 2010)

Surface-emitting polymer laser was fabricated with 1,4-bis[2-[4-[N,N-di(*p*-tolyl)amino]phenyl]vinyl]benzene-doped poly(vinyl-pyrrolidone) thin films sandwiched between two distributed Bragg reflector (DBR) mirrors. Under pulsed optical pumping, Fabry–Perot (FP) type resonance resulted in multi-mode laser oscillations depending upon the active film thickness. With increasing excitation wavelengths, an emission peak based on stimulated resonant Raman scattering (SRRS) was superimposed on the multimode band region. When the SRRS peak just overlapped with one of the FP modes, the emission intensity was enhanced and the line width was considerably narrowed. Such SRRS-coupled FP oscillations can be applied to realize a tunable single-mode surface-emitting polymer laser. © 2010 American Institute of Physics. [doi:10.1063/1.3459967]

Polymer lasers and optical amplifiers will be indispensable for future photonic networks constructed with easy-handled and low-cost plastic optical fibers (POFs) in short range communications. The broad visible emissions of π -conjugated polymers and dye-doped polymers cover the wavelength gaps among the laser diodes and it can be well matched to the lowest light-loss waveguiding region of the POF around 500–600 nm. Various types of optically pumped polymer lasers have been so far reported to meet such mid-visible wavelengths by using distributed feedback (DFB),^{1–3} microdisk⁴ and microring⁵ resonators. The DFB laser is widely employed since its tunable single-mode oscillation is simply attained by thin film coating on a grating substrate with desired spacing. On the other side, the microdisk/ring lasers give rise to multimode lasing. In order to selectively pick up one single-mode oscillation among the multimode lasing, we have been proposing tunable coupling with stimulated resonant Raman scattering (SRRS) in the π -conjugated polymer and doped dye.^{6,7}

Stimulated Raman scattering (SRS) provides mirrorless light amplification as realized in fiber Raman amplifiers in which a tunable gain is obtained at any wavelength accompanied with Raman shifts of the incident light by quartz phonons. Moreover, a compact Raman laser has been researched by means of the SRS with an on-tip silicon waveguide.^{8,9} However, those SRS gains are quite low due to its off-resonant Raman process, therefore, a long fiber length and a feedback cavity are required for the FRA and the Si Raman laser, respectively. On the other hand, the optical amplification by SRRS can be obtained with tiny molecular crystals as first found for anthracene¹⁰ and then for thiophene/phenylene co-oligomer crystals.^{11,12} The resonant electronic excitation and efficient light confinement in the low-dimensional crystal enhance the Raman amplification even in a submillimeter-scale cavity. Similar SRRS phenomena have also been found for π -conjugated polymer^{13–15} and

dye-doped polymer films.¹⁶ Under resonant excitation at their absorption edge, the emission peak Raman-shifted by the π -conjugated backbone stretching appears in the wavelength region where the amplified spontaneous emission (ASE) band overlaps. However, their SRRS intensity is considerably weak and its peak width is broad as compared with that taken from the low-molecular crystals due to random orientation of polymer chains.

When those polymer films are incorporated with DFB and microring resonators,^{6,7} the SRRS intensity can be enhanced with reduced peak width and ASE background by coupling with their laser modes. In particular, a selective coupling of the SRRS peak with one of the multimode microring oscillations envisages us to realize a single-mode polymer Raman laser. However, the decoupling of the emission from the microring cavity is not suitable for simple light coupling into POFs. As a polymer laser to meet such issues, surface-emitting devices with a Fabry–Perot (FP) type resonator have demonstrated a low-threshold lasing and a compact integrated system with LD pumping.^{17,18} In this work, therefore, a surface-emitting FP-type laser is fabricated with dye-doped polymer films using distributed Bragg reflector (DBR) mirrors, and the SRRS-coupled lasing is studied.

As a laser dye molecule, 1, 4-bis[2-[4-[N,N-di(*p*-tolyl)amino]phenyl]vinyl]benzene (DADSB) was used and dissolved in a 10 wt % chloroform solution of poly(vinyl-pyrrolidone) (PVP). Their molecular structures are shown in Fig. 1(a). The DADSB concentration was 3.6 wt % to PVP. The DADSB/PVP solution was spin-coated on a DBR mirror surface typically at a rotation speed of 1000 rpm for 20 s. Then, another DBR mirror was faced down onto the coated surface. Dryness at 80 °C for 5 min in an air oven yielded a DADSB/PVP film sandwiched between the two DBR mirrors as schematically shown in Fig. 1(b). The thickness of the DADSB/PVP film was changed by different loading onto the top DBR mirror during dryness.

The DBR mirror used was made by multilayered dielectric sputtering of SiO₂/TiO₂ on a quartz substrate (10 × 10

^{a)}Electronic mail: yanagi@ms.naist.jp.

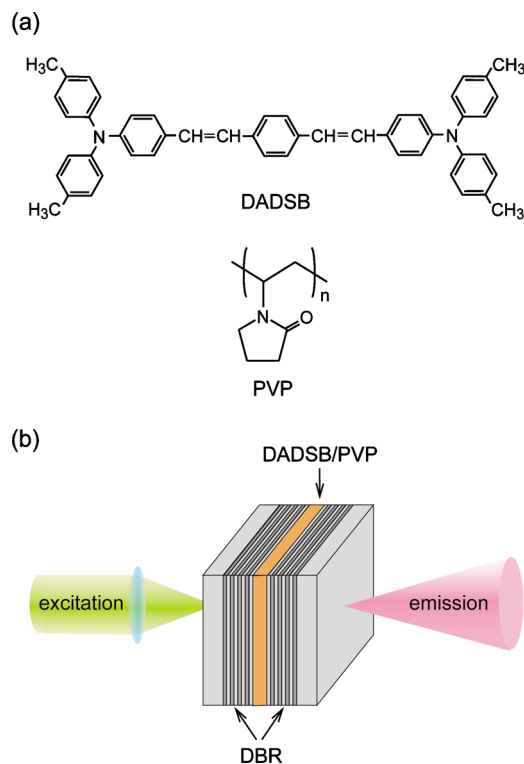


FIG. 1. (Color online) Molecular structures of DADSB and PVP (a), and schematic of surface-emitting FP structure with DADSB/PVP active film sandwiched between DBR mirrors (b).

$\times 1 \text{ mm}^3$). Nine pairs of SiO_2 (235 nm thick) and TiO_2 (65 nm thick) were alternately coated as is shown in a scanning electron micrograph in Fig. 2(a). The transmission spectra of the prepared DBR mirror is shown in Fig. 2(b) together with the absorption and fluorescence spectra of the DADSB/PVP film coated on glass as a reference. The transmittance is $>70\%$ in the absorption region at $\lambda < 480 \text{ nm}$ while the reflectance of $>99.5\%$ is obtained in the fluorescence band

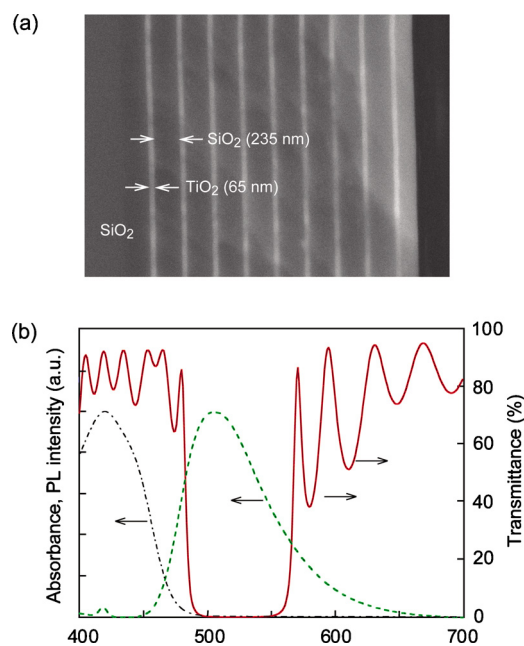


FIG. 2. (Color online) Cross-sectional scanning electron micrograph of the DBR mirror (a) and its optical transmission spectrum (solid line) together with absorption (dotted-dashed line) and fluorescence (dashed line) spectra (b).

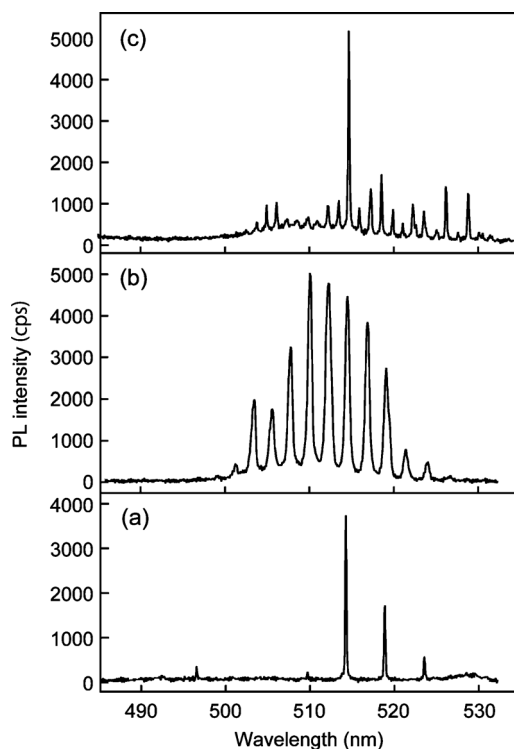


FIG. 3. Optically pumped PL spectra of the surface-emitting FP structures with DADSB/PPV films having different thicknesses. λ_{ex} is 440.6 (a), 441.0 (b), and 454.2 nm (c).

region at $498 < \lambda < 549 \text{ nm}$. Optically pumped photoluminescence (PL) spectra were taken under pulsed excitation using a frequency variable YAG/OPO laser (pulse duration $\sim 5 \text{ ns}$, repetition rate 10 Hz) at room temperature. The excitation beam with a spot size $< 1 \text{ mm}$ was vertically incident onto the back side of one DBR mirror and the emission escaped from the backside of another DBR was detected with a charge coupled device (CCD) spectrometer as shown in Fig. 1(b). A low-pass filter was set in front of the CCD spectrometer to cut the excitation beam. The wavelength resolution of the spectrometer with a 1200 gratings/mm is 0.15 nm.

A reference DADSB/PVP film coated on glass exhibited an ASE band around $\lambda = 510 \text{ nm}$ with a full width of half maximum (FWHM) of $\sim 9 \text{ nm}$ when the edge emission from the film was collected in the direction parallel to the film surface under excitation at $\lambda_{\text{ex}} < 460 \text{ nm}$. With increasing λ_{ex} , an additional peak by SRRS (FWHM $\sim 0.5 \text{ nm}$) appeared in the ASE band region and its peak position shifted to the longer wavelengths according to λ_{ex} . The Raman shift was kept at $\sim 1600 \text{ cm}^{-1}$ which was assigned to the π -conjugated stretching vibration of the DADSB molecule. On the other hand, the emission collected in the direction normal to the film surface was very weak with a broad fluorescence spectrum.

When the DADSB/PVP film was sandwiched between the DBR mirrors, a variety of FP mode lasing was observed depending upon the film thickness as shown in Fig. 3. A thin DADSB/PVP film exhibited a couple of emission peaks under excitation at $\lambda_{\text{ex}} = 441 \text{ nm}$ as shown in Fig. 3(a). With increasing film thickness, the number of the FP mode peaks increased as shown in Figs. 3(b) and 3(c). Their thicknesses were estimated to be $18 \mu\text{m}$, $37 \mu\text{m}$, and $64 \mu\text{m}$ for the films in Figs. 3(a)–3(c), respectively, according to the equa-

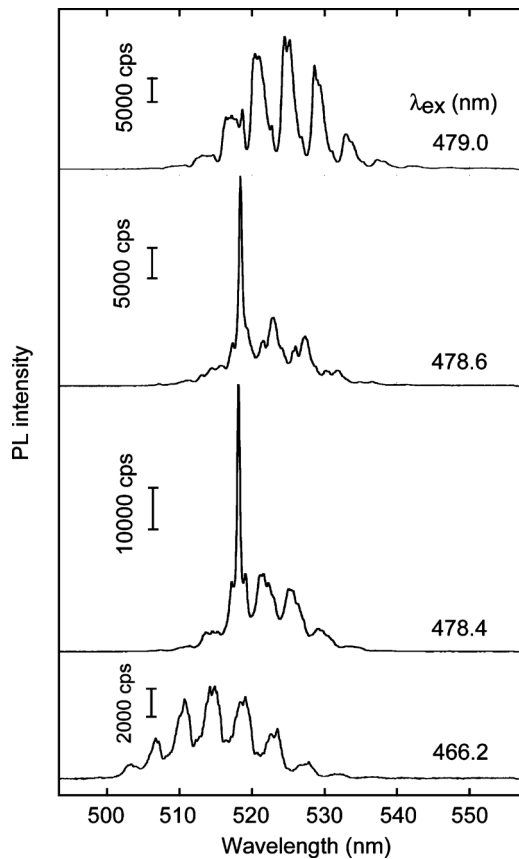


FIG. 4. PL spectral changes of optically pumped surface-emitting FP structure as a function of λ_{ex} .

tion, $L=1/(2n\Delta\nu)$, where L is the cavity length, n is the refractive index of the film and $\Delta\nu$ is the mode interval in frequency. The n of the DADSB/PVP film was measured to be 1.57 around $\lambda=510$ nm by using spectroscopic ellipsometry.

When the λ_{ex} was shifted to the longer wavelengths close to the absorption edge of the DADSB/PVP film, the PL spectra taken from the FP structure changed with an overlapped SRRS peak as shown in Fig. 4. At $\lambda_{\text{ex}}=466.2$ nm, FP multimode peaks corresponding to a cavity length of ~ 20 μm appeared at $\lambda=500$ – 530 nm. Their peak width is considerably broad as compared with those shown in Fig. 3 because the thickness of the DADSB/PVP film is not homogeneous. When the λ_{ex} was increased to 478.4 nm, the multimode peaks shifted to the longer wavelengths at $\lambda=510$ – 535 nm due to the self-absorption effect. Under less excitation at the longer λ_{ex} , the absorption tail causes the redshift in the ASE band to lower the self-absorption. Note that an intense peak is appeared at $\lambda=518.1$ nm overlapping with one of the FP modes. This amplified peak is assigned to SRRS with the Raman shift of 1602 cm^{-1} . A slight shift to $\lambda_{\text{ex}}=478.6$ nm still gives rise to the SRRS peak at $\lambda=518.4$ nm although its intensity is reduced to about half. When λ_{ex} is further increased to 479.0 nm, the SRRS peak became very weak at 518.6 nm locating on the shoulder of the FP mode. These spectral changes reveal that the SRRS is enhanced when its Raman-shifted wavelength is just coupled with the FP mode peak, and tunable surface-emitting lasing by SRRS/FP coupling is attained even from such an inhomogeneous film.

This coupling effect was evaluated with the quality factor Q calculated from $Q=\nu/\Delta\nu$ where ν and $\Delta\nu$ are the frequency and the FWHM of the SRRS peak. The Q values of the FP-coupled SRRS peaks at $\lambda_{\text{ex}}=478.4$ and 478.6 nm in Fig. 4 are 1400 and 1178, respectively. The value, in particular obtained at the former well-coupled frequency, is meaningfully higher than $Q=1003$ estimated for the SRRS peak of the reference DADSB/PVP film on glass. This Q value corresponding to the SRRS in the slab waveguide is dependent on the Raman broadening but less sensitive to the film quality. Therefore, we conclude that the increase in the Q value in the coupled peak is synergetic effect of the SRRS with the FP lasing mode.

In summary, we have fabricated a surface-emitting dye-doped polymer laser with the DBR-sandwiched FP cavity. By tuning the excitation wavelength to which the SRRS peak just couples with one of the FP lasing modes, the emission peak was considerably gain-narrowed with an improved Q factor. In the present study, such SRRS/FP coupling was not attained with homogeneous films as shown in Fig. 3, since the FP peaks usually disappeared at longer λ_{ex} where the resonant absorption became very weak. Furthermore, this coupling effect was demonstrated only at one FP mode peak, since the large Stokes shift in DADSB prevents the efficient SRRS from being coupled with the FP mode at the longer wavelengths. With more suitably designed spectral conditions for resonant excitation and precise cavity structures, we could realize tunable single-mode lasing from such a simple surface-emitting polymer device.

¹C. Kallinger, M. Hilmer, A. Haugeneder, M. Perner, W. Spirkl, U. Lemmer, J. Feldmann, U. Scherf, K. Müllen, A. Gombert, and V. Wittwer, *Adv. Mater. (Weinheim, Ger.)* **10**, 920 (1998).

²K. Yamashita, M. Arimatsu, M. Takayama, K. Oe, and H. Yanagi, *Appl. Phys. Lett.* **92**, 243306 (2008).

³K. Yamashita, M. Arimatsu, N. Takeuchi, M. Takayama, K. Oe, and H. Yanagi, *Appl. Phys. Lett.* **93**, 233303 (2008).

⁴T. Nakao, H. Tanaka, Y. Yoshida, N. Tsujimoto, A. Fujii, and M. Ozaki, *Thin Solid Films* **516**, 2767 (2008).

⁵H. Tanaka, Y. Yoshida, T. Nakao, N. Tsujimoto, A. Fujii, and M. Ozaki, *Jpn. J. Appl. Phys., Part 2* **45**, L1077 (2006).

⁶H. Yanagi, N. Kawazu, R. Takeaki, S. Tomita, K. Yamashita, and K. Oe, *Synth. Met.* **159**, 802 (2009).

⁷H. Yanagi, R. Takeaki, S. Tomita, A. Ishizumi, F. Sasaki, K. Yamashita, and K. Oe, *Appl. Phys. Lett.* **95**, 033306 (2009).

⁸H. Rong, A. Lin, R. Jones, O. Cohen, D. Hak, R. Nicolaescu, A. Fang, and M. Paniccia, *Nature (London)* **433**, 292 (2005).

⁹H. Rong, A. Lin, R. Jones, O. Cohen, D. Hak, A. Fang, and M. Paniccia, *Nature (London)* **433**, 725 (2005).

¹⁰A. A. Maksimov and I. I. Tartakovski, *Phys. Status Solidi B* **107**, 55 (1981).

¹¹H. Yanagi, A. Yoshiki, S. Hotta, and S. Kobayashi, *Appl. Phys. Lett.* **83**, 1941 (2003).

¹²H. Yanagi, A. Yoshiki, S. Hotta, and S. Kobayashi, *J. Appl. Phys.* **96**, 4240 (2004).

¹³M. N. Shkunov, W. Gellermann, and Z. V. Vardeny, *Appl. Phys. Lett.* **73**, 2878 (1998).

¹⁴H. Yanagi, T. Murai, and S. Fujimoto, *Appl. Phys. Lett.* **89**, 141114 (2006).

¹⁵S. Fujimoto, S. Tomita, and H. Yanagi, *Jpn. J. Appl. Phys.* **47**, 1188 (2008).

¹⁶I. Sakata, S. Fujimoto, and H. Yanagi, *Appl. Phys. Lett.* **88**, 191104 (2006).

¹⁷T. Granlund, M. Theander, M. Berggren, M. Andersson, A. Ruzbeckas, V. Sundström, G. Björk, M. Granström, and O. Inganäs, *Chem. Phys. Lett.* **288**, 879 (1998).

¹⁸H. Sakata and H. Takeuchi, *Appl. Phys. Lett.* **92**, 113310 (2008).